Vibro-acoustics of porous materials - waveguide modelling approach

R Darula and S Sorokin

Department of Mechanical and Manufacturing Engineering, Aalborg University, Fibigerstraede 16, Aalborg East 9220, DK

E-mail: dra@m-tech.aau.dk

Abstract. The porous material is considered as a compound multi-layered waveguide (i.e. a fluid layer surrounded with elastic layers) with traction free boundary conditions. The attenuation of the vibro-acoustic waves in such a material is assessed. This approach is compared with a conventional Biot's model and a qualitative agreement in phase velocities as well as damping estimates is found. The waveguide model predicts four waves, out of which two are attenuated when the viscous fluid is considered (while the elastic layer being ideally lossless). One of these waves is found to be significantly controlled by the fluid viscosity, while for the other the effect of viscosity was observed for very small frequencies. The Biot's model predicts only one of these attenuated waves, where the latter one is not predicted. Thus the proposed waveguide approach provide additional information about the wave propagation in porous materials.

1. Introduction

Propagation and attenuation of waves in two-phase waveguides such as porous elastic materials saturated with air or water has been a subject of thorough analysis for decades. The generally recognised model of these phenomena has been proposed by M.A. Biot in the classical papers [1, 2]. This model has found its applications in many fields of engineering from material science and soil mechanics to acoustics [3, 4]. Its predictions are known to be fairly accurate provided that the empirical constants are available from series of experiments. Furthermore, some parameters involved in the formulation of the Biot's model, such as an apparent mass, need to be determined in an indirect way. Therefore, many variations and modifications have been proposed (e.g., [4, 5, 6]) in order to get rid of some drawbacks. However, all these models are based on the original Biot's concept and empirical parameters of a given porous material need to be found from dedicated experiments.

In this article, we consider the canonical problem of low-frequency wave propagation in a three-layered medium consisting of two phases: an elastic solid and a viscous fluid. The dissipative properties of the fluid are characterised by a single parameter, its kinematic viscosity, which is well known. Furthermore, since we are interested in fluid induced attenuation, no internal losses are assumed in the structural part, i.e. ideally elastic layers are considered. The purpose of this modelling is to see the resemblances as well as differences with the Biot's model in dispersion diagrams within low frequencies. On the top of that we are aiming also at comparison of the damping estimation obtained with either of the model.

We assess damping for the branches of dispersion diagrams with zero cut-on frequencies, i.e. in the low-frequency regime. We adopt the following convention - $\exp(kx - i\omega t)$. The damping

Content from this work may be used under the terms of the Creative Commons Attribution 3.0 licence. Any further distribution of this work must maintain attribution to the author(s) and the title of the work, journal citation and DOI.
Published under licence by IOP Publishing Ltd

is estimated for a given frequency ω from the wavenumbers k, taking the ratio of their real and imaginary parts, i.e. the wave attenuation in the space domain is assessed.

The main motivation to explore waveguide properties of a three-layered medium versus the Biot's model is a rational problem formulation. On one hand the proposed approach requires fewer parameters than the Biot's model. These parameters have simple meaning and are easy to be determined experimentally. On the other hand it provides an insight into physics of propagation of waves in a porous material.

2. Model derivation

We consider a layer of fluid of height $2h_F$ inserted between two identical elastic layers of thickness $t_E = h_S - h_F$, as shown in figure 1. The outer boundaries are set free to move. Furthermore, we solve the problem in the plane-strain formulation and analyse the symmetric and skew symmetric wave modes separately.

The governing equations are written in a non-dimensional form, where parameters used are explained in table 1. To de-couple the wave motion into dilatational and shear components, a displacement field in solid and velocity field in fluid are expressed via potentials, i.e. Lame (or Kirchhoff) decomposition is applied.

The non-dimensional form of governing equations of the wave propagation in the elastic layer is [7]

$$\nabla^2\phi_S + \Omega_S^2\phi_S = 0, \tag{1}$$

$$\nabla^2\psi_S + \frac{\Omega_S^2}{\zeta_{S,21}^2}\psi_S = 0, \tag{2}$$

where displacement potentials are $\phi_S(x,z)$ and $\psi_S(x,z)$.

The fluid phase is modelled using the linearised Navier-Stokes equations, which can be

Table 1. Parameters used.

Name	Expression	Name	Expression	Name	Expression
Solid wave spd.(x)	$c_{S,1}$	Solid wave speed(z)	$c_{S,2}$	Fluid wave speed	c_F
Frequency	ω	Half of waveguide hght.	h_S	Half of fluid height	h_F
Viscosity	ν	Density of solid	ρ_S	Density of fluid	ρ_F
Nondim.height	$h_{FS} = \frac{h_F}{h_S}$	Solid speed ratio	$\zeta_{S,21} = \frac{c_{S,2}}{c_{S,1}}$	Fluid-solid speed rt.	$\zeta_{FS,1} = \frac{c_F}{c_{S,1}}$
Density ratio	$\eta_{FS} = \frac{\rho_F}{\rho_S}$	Nondim.viscosity	$\kappa_{FS} = \frac{\nu}{h_S c_{S,1}}$	Scaled frequency	$\Omega_S = \frac{\omega h_S}{c_{S,1}}$

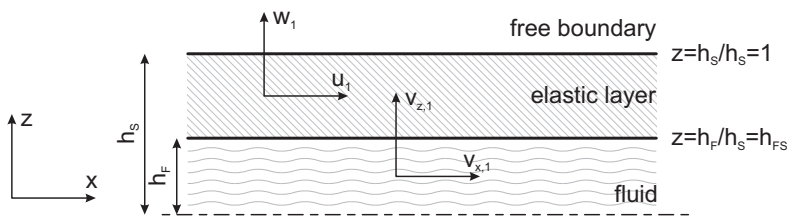

Figure 1. Assumed fluid-structure problem.

transformed into the form of fluid velocity potentials as in [8]

$$\nabla^2\phi_F + \frac{\Omega_S^2}{\zeta_{FS,1}^2}\phi_F = 0, \tag{3}$$

$$\kappa_{FS}\nabla^2\psi_F + i\Omega_S\psi_F = 0, \tag{4}$$

with fluid velocity potentials $\phi_F(x,z)$ and $\psi_F(x,z)$. One can notice, that the equation for shear potential (equation 4) is a diffusion type equation, i.e. responsible for attenuation of wave propagation.

For the free boundaries (i.e. at $z = 1$, figure 1), the condition of zero stresses (the normal and shear one) is taken [7]

$$\sigma_z = \lambda\left(\frac{\partial^2\phi_S}{\partial x^2} + \frac{\partial^2\phi_S}{\partial z^2}\right) + 2\mu\left(\frac{\partial^2\phi_S}{\partial z^2} + \frac{\partial^2\psi_S}{\partial x\partial z}\right) = 0, \tag{5}$$

$$\tau_{xz} = \mu\left(2\frac{\partial^2\phi_S}{\partial x\partial z} - \frac{\partial^2\psi_S}{\partial z^2} + \frac{\partial^2\psi_S}{\partial x^2}\right) = 0, \tag{6}$$

Furthermore, at interfaces of the two media (at $z = h_{FS}$, figure 1) the velocities and stresses of both media need to be in equilibrium [7, 8]

$$-i\Omega_S\left(\frac{\partial\phi_S}{\partial x} - \frac{\partial\psi_S}{\partial z}\right) = h_{FS}\zeta_{FS,1}\left(\frac{\partial\phi_F}{\partial x} - \frac{\partial\psi_F}{\partial z}\right), \tag{7}$$

$$-i\Omega_S\left(\frac{\partial\phi_S}{\partial z} + \frac{\partial\psi_S}{\partial x}\right) = h_{FS}\zeta_{FS,1}\left(\frac{\partial\phi_F}{\partial z} + \frac{\partial\psi_F}{\partial x}\right), \tag{8}$$

$$\begin{aligned}\nabla^2\phi_S + 2\zeta_{S,12}^2\left(\frac{\partial^2\phi_S}{\partial x^2} + \frac{\partial^2\psi_S}{\partial x\partial z}\right) = ...\\ ...\eta_{FS}h_{FS}\zeta_{FS,1}\left[-\frac{4\kappa_{FS}}{3}\nabla^2\phi_F - i\Omega_S\phi_F + \kappa_{FS}\left(\frac{\partial^2\phi_F}{\partial^2 z} + \frac{\partial^2\psi_F}{\partial x\partial z}\right)\right],\end{aligned} \tag{9}$$

$$\zeta_{S,12}\left(2\frac{\partial^2\phi_S}{\partial x\partial z} + \frac{\partial^2\psi_S}{\partial x^2} - \frac{\partial^2\psi_S}{\partial z^2}\right) = \eta_{FS}h_{FS}\zeta_{FS,1}\kappa_{FS}\left[2\frac{\partial^2\phi_F}{\partial x\partial z} + \frac{\partial^2\psi_F}{\partial x^2} - \frac{\partial^2\psi_F}{\partial z^2}\right]. \tag{10}$$

3. Elastic layer with inviscid fluid

To assess the amount of attenuation introduced by fluid viscosity, a reference model, where viscosity is neglected (i.e. with an undamped fluid considered), needs to be analysed first.

Thus, let us take $\kappa_{FS} = 0$. Then the fluid motion is described purely by acoustic potential ϕ_F, i.e. the interface condition for velocity in x direction (equation 7) is not needed and all the other conditions are modified accordingly. Furthermore, the shear stress in the solid (the right hand side of equation 10) is equal to zero at the solid-fluid interface.

The problem can be solved for both symmetric, as well as skew-symmetric modes separately. Using the parameters, listed in table 2, the dispersion curves are identified and plotted in figure 2.

Table 2. Numerical values of parameters used.

h_{FS}	$\zeta_{S,12}$	$\zeta_{FS,1}$	η_{FS}
0.04	0.503	5.52	0.01

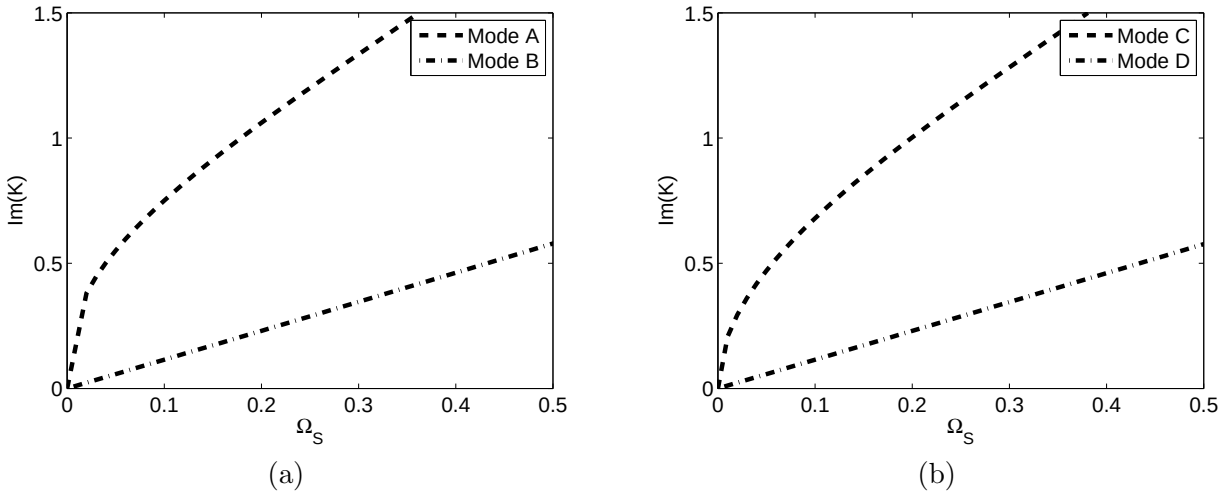

Figure 2. Dispersion curves for an elastic layer with inviscid fluid for (a) the symmetric and (b) the skew-symmetric propagating modes (imaginary parts of wave numbers). The labels A-D are used to mark the modes analysed in section 3.1.

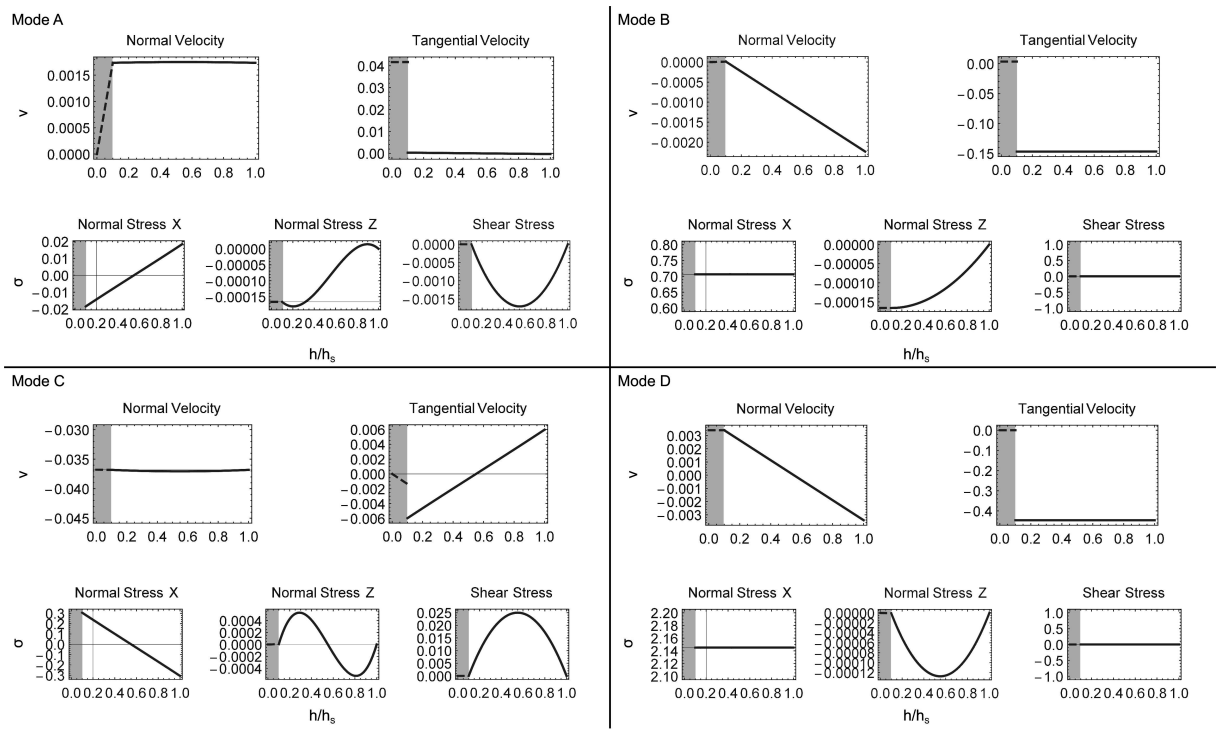

Figure 3. Analysis of the first two symmetric A,B and skew-symmetric modes C,D. Sub-figures present the distribution of velocities and stresses through the layers ($z = h/h_S$) and correspond to modes labelled in dispersion diagrams (figure 2). For illustrative purposes, the value $h_{FS} = 0.1$ is chosen as a border between the fluid and the solid. The fluid layer ($0 \leq h/h_S \leq 0.1$) is highlighted.

3.1. Identification of modes

The dispersion diagrams presented in figure 2 provide only information about temporal and spatial evolution of the mode in the two-phase medium. An additional analysis is required to understand what type of wave motion (e.g. dilatational, bending, shear) each mode represents.

In order to accomplish this task, the normal and tangential velocities, as well as normal and shear stresses need to be analysed for the modes of interest. The stresses (σ, τ) are scaled with respect to squared speed in the solid medium $(c_{S,1}^2)$ and its density (ρ_S), while the velocities (v_n, v_t) are scaled with respect to wave speed in the fluid c_F. Let us pick four points from the dispersion diagram (K_n, Ω_n), one for each mode, and plot the profiles of corresponding velocities and stresses, i.e. functions of the coordinate z. The normal and tangential velocities are found to be in phase each other. Similarly the normal stresses are in phase with velocities, only the shear stress is out of phase (with a phase shift $\pi/2$).

Inspecting the figure 3, one can conclude:

- **Mode A** (symmetric) - dilatational fluid and breathing solid mode - where tangential velocity and normal stress (pressure) in the fluid are present, i.e. the fluid performs a dilatational motion in x-direction. In solid, the normal stress in horizontal (x) direction is dominant and linearly dependent on the coordinate z, while the shear stress is zero at the edges and maximum in the middle of the elastic layer, i.e. so-called breathing bending mode is induced.
- **Mode B** (symmetric) - dilatational solid mode - there is no velocity of the fluid, i.e. the mode is affecting only the elastic layer. The tangential velocity in solid is uniform, while the normal velocity is small at the boundary with fluid and maximal at the free end. Also the normal stress in x-direction is constant, while the shear stress is zero, i.e. the wave in solid is longitudinal.
- **Mode C** (skew-symmetric) - solid bending mode - the normal stresses in x-direction are a linear function of z and the shear stress is zero at the boundaries of the elastic layer and maximal in its middle. Given the constant normal velocity and a linear dependence of the tangential velocity on z, one can conclude that this mode correspond to the bending of the solid layer, where the fluid just follows the solid. This mode is similar to the symmetric mode A, however in the mode A the fluid moves in tangential (x) direction at different speeds across z (i.e. it is squeezed, thus A is a breathing bending mode), while in the mode C the tangential velocity is close to zero.
- **Mode D** (skew-symmetric) - solid skew-symmetric dilatational mode with fluid interaction - the normal velocity in the fluid is constant, i.e. it interacts with solid which moves uniformly in an axial direction, since the normal stress in x-direction is dominant. This mode is similar to the mode B, however in the case of the mode the D the lateral motion of solid is skew symmetric, i.e. the upper and lower solid layers move in antiphase.

A simplified visualization of the modes is shown in figure 4.

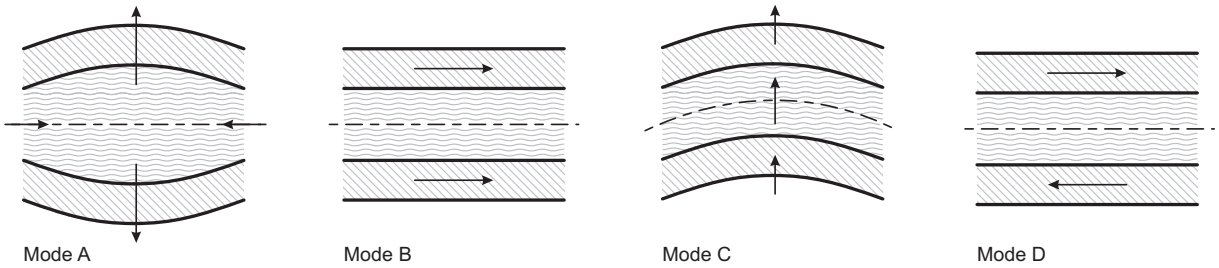

Figure 4. Visualization of the modes.

4. Effects of viscosity

To analyse the damping introduced by the fluid-structure interaction, fluid viscosity is added to the problem analysed. The losses in the solid layer are considered to be small enough to be neglected.

In the model we follow Biot's assumption of Poiseuille flow in a fluid [1, 9] in the course of wave motion. In [1], the upper limit frequency for a stable Poiseuille flow is defined in terms of the width (h) and fluid viscosity (ν)

$$f_l = \frac{\pi\nu}{4h^2}. \tag{11}$$

Using the non-dimensional parameters introduced in table 1, for the plane strain state, the limit frequency can be rewritten as

$$\Omega_l = \frac{\pi^2\kappa_{FS}}{8h_{FS}^2}, \tag{12}$$

where for the parameters listed in table 2 and $\kappa_{FS} = 0.0005$, $\Omega_l = 0.4$. Therefore further on our analysis will be performed in the region $\Omega_S < \Omega_l$.

4.1. Assessment of phase velocities

The dispersion diagrams have already been plotted in figure 2 and they are labelled according to the waves analysed in previous sections.

The corresponding phase velocities (scaled with the velocity for inviscid fluid) for symmetric and skew-symmetric modes are shown in figure 5, where:

- **Modes B - C** - are insignificantly influenced by fluid viscosity, since for the ratio of velocities is valid $v_{visc}/v_{invisc} \approx 1$.
- **Mode D** - is affected by viscosity, however the effect in the range, the model was reliable, is small and we can say that $v_{visc}/v_{invisc} \approx 1$ is valid as well.
- **Mode A** - phase speeds are increasing as the frequency increases. For the parameters chosen (table 2) within the Poiseuille flow the fluid speed is slower than the solid one, i.e. $v_{visc}/v_{invisc} < 1$.

4.2. Assessment of damping

The damping of the waves in the spatial domain is evaluated as a ratio of the real and imaginary components of the corresponding wave-numbers (i.e. $\mathrm{Re}(K)/\mathrm{Im}(K)$), as it is shown in figure 6. From the figure, following observations can be drawn:

- **Modes B-C** - are insignificantly attenuated, which corresponds to the assumption that the solid is treated as ideal with no internal dissipation. Thus one can conclude, that there is no significant interaction of the fluid viscosity with the waves originated in the solid part.
- **Mode D** - a small amount of damping, which is frequency dependent, is observed. For lower frequencies it slightly increases which indicates that it is coupled to the fluid phase and the interface condition. It needs to be noticed that for $\Omega_S \to 0$ the model was not reliable, thus the data are plotted only for $\Omega_S > 0.002$.
- **Mode A** - is the one where the significant damping is observed. There is no attenuation for zero frequency, however increasing the frequency, its amount increases up to some value (for the parameters used it is -0.27) is reached. This corresponds observations presented in [10], where the fluid-borne waves at low frequencies are strongly damped.

5. Influence of viscosity on attenuation level

The wave propagation in either fluid or elastic layer is well known and described in number of textbooks (e.g. [7, 11]). On the other hand, the fluid structure interaction problem is also well established, but from the view point of porous media, there have not been done so many studies. Therefore the parametric study deals with the interaction of the two phases (the fluid and elastic ones) in a wave with a focus on attenuation induced by the fluid viscosity (i.e. treating the elastic solid as ideal with no energy dissipation mechanism).

As we have shown in the previous sections, there are two waves (mode A for symmetric and mode D for skew-symmetric wave), which experience fluid-structure interaction and which are influenced by the fluid's viscosity. The dispersion diagrams and attenuation plots for both waves and for three levels of viscosity (infinitesimally small, i.e. inviscid and $\kappa_{FS} = \{0.0005, 0.005\}$) is shown in figure 7 and one can conclude:

- **Mode A** - figure 7a-b - this wave is significantly affected by the fluid viscosity κ_{FS}. Increasing its value, the real parts of the wavenumber increases. The same can be observed in the imaginary part. Thus defining the attenuation as a ratio of the real to imaginary part of the wavenumber, it becomes frequency dependent, converging to some value (around -0.27 for the set of parameters used) as frequency is reduced. For large frequencies (above

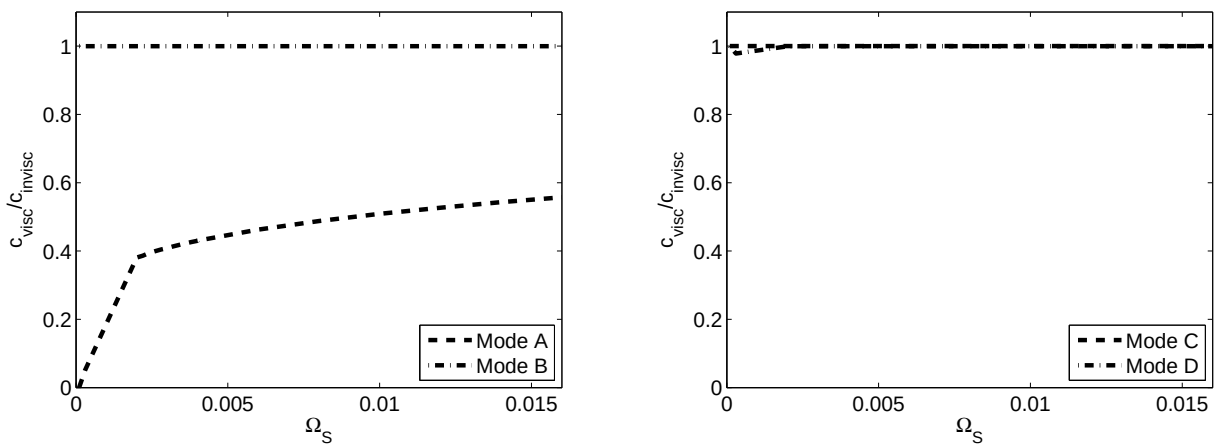

(a) (b)

Figure 5. Comparison of viscous and inviscid phase velocities (v_{visc}/v_{invisc}) for (a) symmetric (A, B) and (b) skew-symmetric modes (C, D).

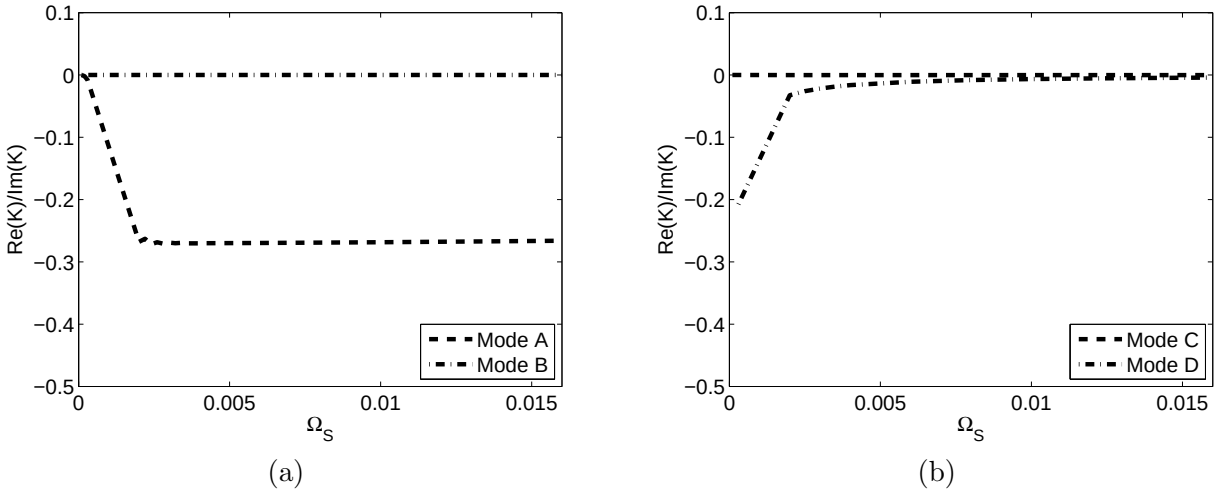

Figure 6. Comparison of attenuation of wave propagation (in terms of a ratio of the real and imaginary parts of the corresponding wave-numbers) for (a) symmetric (A, B) and (b) skew-symmetric modes (C, D).

the Poiseuille flow limit, $\Omega_S = 0.4$ for $\kappa_{FS} = 0.0005$ and $\Omega_S = 4$ for $\kappa_{FS} = 0.005$), the attenuation is converging to zero.

- **Mode D** - figure 7c-d - the real part of the wavenumber is approximately constant over frequency, while the imaginary part is identical to the inviscid one. Therefore the attenuation is negligible for higher frequencies, while are increasing for very small frequencies.

It needs to be noticed that the behaviour of the system at the limit $\Omega_S \to 0$ is beyond the scopes of the article and is left-out for the further analysis.

6. Waveguide vs. Biot's model

As already stated in the introduction, the Biot's model is well established and widely used for wave propagation in porous materials. It is derived under several heuristic assumptions using Lagrange equations. We follow the waveguide modelling approach in order to simplify the problem formulation and therefore to gain some physical in-sight of wave propagation in such materials.

From the previous sections it can be concluded, that both models agree qualitatively in the modelling of the relative phase speeds. The ratio of these speeds for the dilatational wave of the first kind (Mode B) and the rotational wave (Mode C) to their counterparts from the Biot's model are close to 1 (figure 5). The dilatational wave of the second kind (Mode A) is non-linearly dependent on frequency in Biot's model, which qualitatively agrees with the prediction of the waveguide model (figure 5a, Mode A). The same comparison of Biot's and waveguide models holds also for damping.

These results suggest, that although the two models are derived quite differently, the important features of wave propagation in porous medium are captured by both of them. On the other hand, the waveguide model predicts four waves (two dilatational and two rotational ones), whereas Biot's model does not capture the solid shear wave (Mode D). This wave was observed to be also lightly damped (figure 6b), which is a result of the fluid-structure interaction (no damping of elastic part is assumed). Further analysis is needed to come up with any qualifications regarding this discrepancy between Biot's and waveguide models.

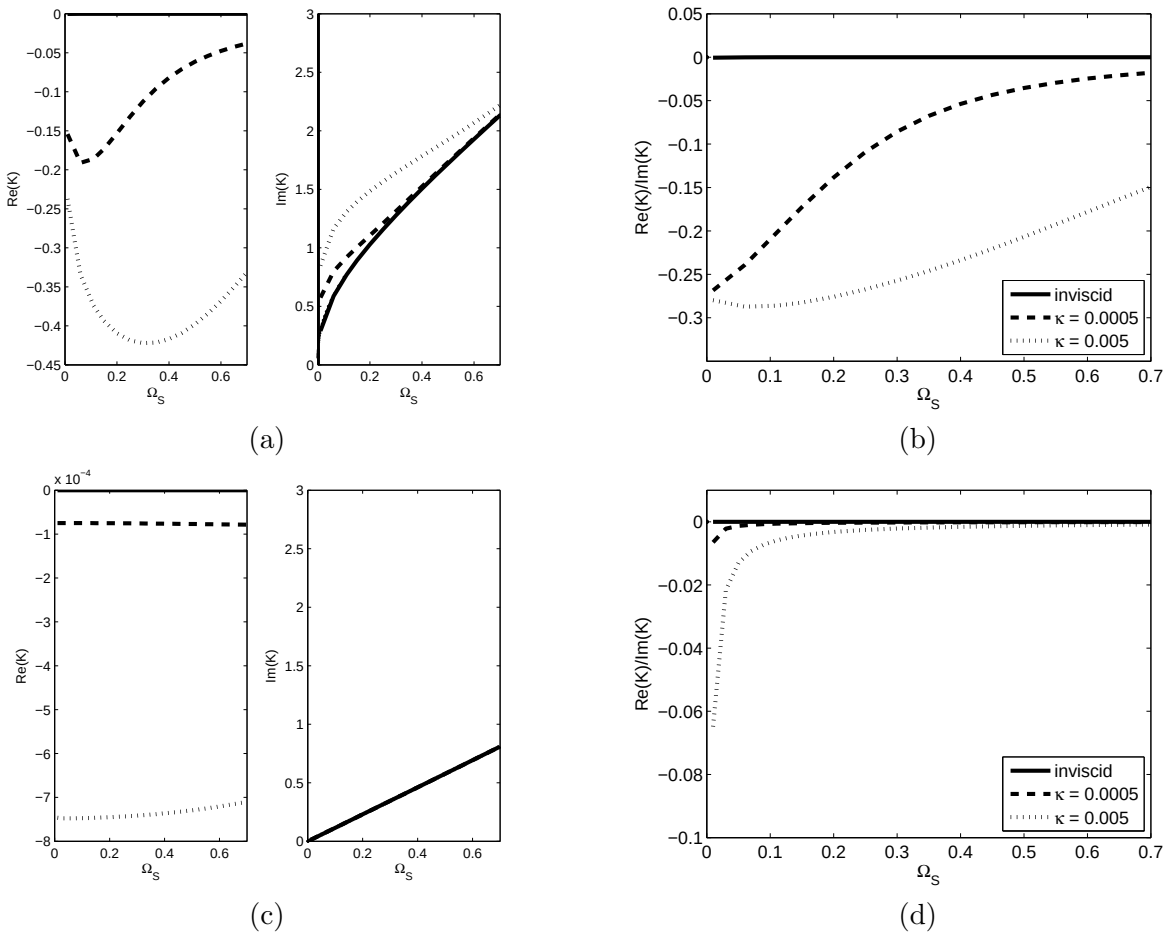

Figure 7. The dispersion diagrams ((a) and (c)) and attenuation plots ((b) and (d)) for viscosity variation of the symmetric mode A (a-b) and the skew-symmetric one D (c-d).

7. Conclusions

In this article a waveguide model of porous media has been derived and discussed. With the waveguide approach we were able to identify the mode types (dilatational/shear/bending) as well as their origin (fluid/solid based) easily. Furthermore the wave speeds and damping (in spatial domain) is assessed directly using the complex valued wavenumbers. The speeds and damping are found to be in a qualitative agreement with Biot's model.

The proposed waveguide model requires as an input just the geometry and material properties of the fluid as well as solid phases, i.e. its characterization is straightforward. Since the waveguide model is capable to predict one more wave, it is considered as a 'higher-order model'. All the encouraging outcomes are planned to be verified also quantitatively as well as experimentally later on in the project.

Acknowledgments

The financial support from DFF, project no.4005-00348, is greatly acknowledged.

References

[1] Biot M A 1956 *J. Acoust. Soc. Am.* **28** (2) 168–178
[2] Biot M A 1956 *J. Acoust. Soc. Am.* **28** (2) 179–191
[3] de Boer R 1998 *Z. Angerw. Math. Mech* **78** 411–466
[4] Dazel O, Brouard B, Depollier C and Griffiths S 2007 *J. Acoust. Soc. Am.* **121** 3509–16
[5] Johnson D L, Koplik J and Dashen R 1987 *J. Fluid Mech.* **176** 379–402
[6] Badia S, Quaini A and Quarteroni A 2009 *J. Comput. Phys.* **228** 7986–14
[7] Achenbach J S 1973 *Wave Propagation in Elastic Solids* (Amsterdam: North-Holland)
[8] Sorokin S V and Chubinskij A V 2008 *J. Sound Vib.* **311** 1020–38
[9] Happel J and Brenner H 1983 *Low Reynolds Number Hydrodynamics* (The Hague: Springer)
[10] Allard J F and Atalla N 2009 *Propagation of Sound in Porous Media: Modelling Sound Absorbing Materials* 2nd ed (Chichester: John Wiley & Sons)
[11] Landau L D and Lifshitz E M 1987 *Fluid mechanics* 2nd ed (Oxford: Pergamon Press)